

Spectral Methods and Running Scales in Causal Dynamical Triangulations

Giuseppe Clemente,^{1,*} Massimo D’Elia,^{1,†} and Alessandro Ferraro^{1,‡}

¹*Dipartimento di Fisica dell’Università di Pisa and INFN - Sezione di Pisa, Largo Pontecorvo 3, I-56127 Pisa, Italy.*

The spectrum of the Laplace-Beltrami operator, computed on the spatial slices of Causal Dynamical Triangulations, is a powerful probe of the geometrical properties of the configurations sampled in the various phases of the lattice theory. We study the behavior of the lowest eigenvalues of the spectrum and show that this can provide information about the running of length scales as a function of the bare parameters of the theory, hence about the critical behavior around possible second order transition points in the CDT phase diagram, where a continuum limit could be defined.

Introduction - The quest for a self-consistent Quantum Theory of Gravity is still far from being settled. Field theoretical approaches are not able to provide a theory which is renormalizable from a standard perturbative point of view, i.e. where all ultraviolet (UV) divergences are reabsorbed at all orders in the coupling expansion by the addition of a finite number of counterterms [1]. However, the idea that a non-perturbative solution could still be found within Quantum Field Theory has not yet been given up, a promising approach being represented by the so-called *asymptotic safety* program [2].

The program is rooted in the renormalization group (RG) framework: in a few words, the idea of asymptotic safety is to find a non-perturbative UV fixed point in the space of possible parameters, with an RG-flow line stemming from it and reproducing the theory of gravity at lower energy scales. Consistent progress has been achieved along this direction by approaches studying the RG-flow [3–6].

A different and complementary approach to the above program is numerical: one considers a discretization of the Euclidean path integral of the theory in configuration space, suitable to be investigated by Monte-Carlo simulations, and looks for possible critical points, i.e. for values of the bare parameters where the correlation length, measured in units of the elementary discretization scale, diverges. Such points are candidate UV fixed points where a continuum limit for QG could be taken.

A standard discretization is based on the Regge formalism [7]: space-time configurations (triangulations) are represented by the possible collections of flat simplexes, glued together so as to reproduce different possible geometries. Pioneering work in this direction has been done by the approach called Dynamical Triangulations [8–12]. In the particular approach known as Causal Dynamical Triangulations (CDT) [13–19], the causal condition of global hyperbolicity [20, 21] is additionally enforced on triangulations by means of a space-time foliation, with spatial slices characterized by a fixed topology (usually S^3), and typically periodic boundary conditions (p.b.c.) in the time direction.

Such configurations are then sampled according to a discretized version of the candidate continuum action. In absence of matter fields, the simplest candidate is the

Einstein-Hilbert action, whose discretized version reads

$$S_E = -k_0 N_0 + k_4 N_4 + \Delta(N_4 + N_{41} - 6N_0), \quad (1)$$

where N_0 , N_4 and N_{41} count respectively the total number of vertices, of generic pentachorons and of special pentachorons having four vertices on the same spatial slice, while k_4 , k_0 and Δ are free dimensionless parameters, related to the *Cosmological* and *Newton* constants Λ and G , and to the freedom in the choice of the time/space asymmetry. Triangulations are then sampled according to a distribution $\propto e^{-S_E}$, with the caveat that k_4 is usually traded for a target volume V , by adding to S_E a volume fixing term (see Ref. [13] for more details).

In this context, a rich phase structure has been found [13, 15, 17, 18, 22], characterized by four different phases, named respectively A , B , C_{dS} (*de Sitter*) and C_b (*bifurcation*). In the B phase, V_S is concentrated almost in a single slice, while both the C_{dS} and the C_b phase are characterized by a more regular spatial volume distribution, localized in a so-called “blob” with a finite time extension; finally, phase A configurations are characterized by multiple and uncorrelated peaks in the spatial volume per slice time $V_S(t)$. The bifurcation phase is further differentiated from the C_{dS} phase by the presence of two different classes of slices which alternate each other in Euclidean time [17, 18, 23].

The transition lines separating the different phases are the candidate places where to search for a continuum limit, especially if they are second order. A candidate transition line, in this respect, is the one separating the C_b from the C_{dS} phase. However, one of the major problems of the CDT program is to find suitable order parameters capable of capturing the essential geometrical features around the transition. Progress in this direction has been achieved by the study of diffusion processes on the triangulations [24, 25], leading to relevant information such as the *spectral dimension* of the triangulations. A generalization along this direction has been proposed in Ref. [26], consisting in the analysis of the spectrum of the Laplace-Beltrami (LB) operator computed on the triangulations.

The analysis of Ref. [26], limited to the LB operator defined on spatial slices, has shown that the various phases can be characterized by the presence (B) or absence (A ,

C_{dS}) of a gap in the spectrum, while the C_b phase shows the alternance of spatial slices of both types, gapped and non-gapped, which for this reason can be named B -type and dS -type slices. The presence of a gap indicates that spatial slices are characterized by a high connectivity and can be interpreted geometrically as a Universe with an infinite dimensionality at large scales, whose diameter grows at most logarithmically as $V_S \rightarrow \infty$. On the contrary, the closing of the gap can be interpreted as the emergence of an extended Universe with a standard finite dimensionality at large scales. In the C_b phase, the alternating slices seem to share similar geometries up to some finite length, then differentiating at larger scales. Moreover, the value of the gap seems to change continuously moving from the B to the C_b phase, then approaching zero towards the C_{dS} phase.

The findings reported above, and the fact that the gap in the spectrum of the LB operator is actually a physical quantity with mass dimension two (hence an inverse squared length), suggest that it can be used as an order parameter to better investigate the $C_b - C_{dS}$ transition and, in case it is second order, to characterize the critical behavior around it. Having this in mind, the purpose of this study is to put the strategy of Ref. [26] on a more quantitative level, studying the infinite volume limit of the gap and its behavior as the transition is approached. Moreover, we will show that one can actually find several length scales, all showing a similar scaling.

Numerical setup - We have investigated CDT with p.b.c. in the Euclidean time direction and an S^3 topology for spatial slices. Configurations have been sampled proportionally to $\exp(-S_E)$ by means of a Metropolis-Hastings algorithm, consisting in a set of local moves (see Ref. [13] for more details). $N_t = 80$ total space-time slices have been taken in all simulations, and the total spatial volume $V_{S,tot} = N_{41}/2$ has been fixed by adding to S_E a term $\Delta S = \epsilon(N_{41} - \bar{N}_{41})^2$, with $\epsilon = 0.005$, then selecting only configurations with exactly the given target volume $\bar{N}_{41}/2$.

We have considered the spatial slices of those configurations, consisting of sets of glued tetrahedra, and computed the eigenvalues of the LB operator discretized on them. As in Ref. [26], the discretization consists of a linear operator L acting on real functions defined on the vertices of the dual graph associated with the triangulation. Since any tetrahedron is adjacent to exactly 4 neighboring tetrahedra, dual graphs are 4-regular (each vertex is connected with other 4 vertices), so that L can be written as $L = 4 \cdot \mathbb{1} - A$ where A is the so-called adjacency matrix, having non-zero unit elements only between pairs of connected vertices. In practice, because of this simple form, it suffices to compute the eigenvalues of A , which is a sparse matrix, and this has been done by means of the ‘Armadillo’ C++ library [27] with Lapack, Arpack and SuperLU support.

The smallest eigenvalue is always $\lambda_0 = 0$, and corre-

sponds to a uniform eigenfunction. Then, λ_1 defines the gap of the spectrum. In the following we will study λ_1 and a few other lowest lying eigenvalues as a function of the spatial volume V_S , trying to extrapolate the $V_S \rightarrow \infty$ (thermodynamical) limit for each of them. For a regular, extended geometry one expects $\lambda_n \rightarrow 0$ in the thermodynamical limit for any finite n , in particular $\lambda_n \propto 1/D^2$ where D is *diameter* of the graph (maximum over all pairs of vertices of the minimum path length connecting the pair).

We have performed sets of simulations at fixed k_0 and different values of Δ , chosen so as to stay in the C_b phase but approaching the C_{dS} phase; moreover, different values of \bar{N}_{41} have been considered, to explore the impact on results of the total spatial volume. A few simulations in the B phase or in the C_{dS} phase have also been performed, to have a comparison for the infinite volume behavior of the lowest lying eigenvalues in those cases.

Results - We start by analyzing the thermodynamical limit of the lowest lying part of the LB spectrum in the C_{dS} phase. To that purpose, we have considered a simulation performed for $k_0 = 0.75$, $\Delta = 0.7$, where the total spatial volume has been fixed to $V_{S,tot} = 4 \cdot 10^4$ (40K). Since for each configuration most of the spatial volume is distributed over many connected slices forming the so-called blob, the volume V_S of single spatial slice is regularly distributed over a wide range going up to a few thousands tetrahedra. Because of our finite sample, consisting of about 500 configurations, this range has been divided in regular bins of volumes, so as to have sufficiently populated subsamples in each bin. Average values $\langle \lambda_n \rangle$ have then been computed over each bin, and results for $n = 1, 3, 5$ are reported in Fig. 1, statistical errors have been computed by properly taking into account autocorrelations among triangulations in the sample. For a few bins, we have reported also results obtained by fixing a different value of $V_{S,tot}$ (60K), to check that this has no impact on the study of the spatial thermodynamical limit.

In the figure we also report best fits according to a power law behavior

$$\langle \lambda_n \rangle = A_n V_S^{-2/d_{EFF}}, \quad (2)$$

all yielding reasonable values of the reduced $\chi^2/\text{d.o.f.}$ and values of $d_{EFF} \simeq 1.6$, in agreement with the spectral effective dimension of spatial slices at large scales measured in previous studies [26, 28]; similar results are obtained for n up to a few tens. This confirms that, in the C_{dS} phase, the gap of the LB operator closes in the thermodynamical limit, with a scaling compatible with the effective spectral dimension at large distances.

The situation is quite different in phase B . In this case, most of the total spatial volume is found in a single slice, so that, in order to study the thermodynamical limit of the spectrum, we had to perform simulations at different values of $V_{S,tot} = 3\text{K}, 4\text{K}, 5\text{K}, 6.5\text{K}, 8\text{K}$. Results

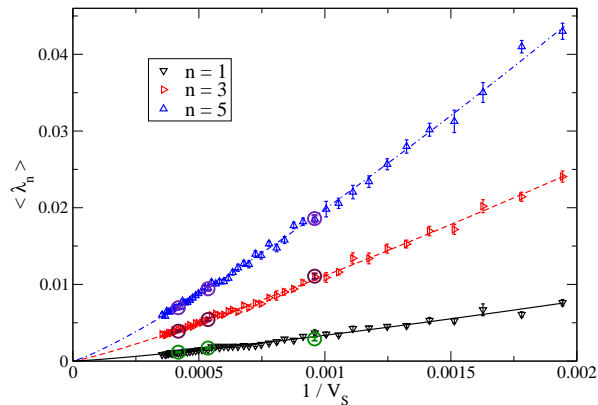


FIG. 1. Average eigenvalues of the LB operator on spatial slices as a function of $1/V_S$ in phase C_{ds} ($k_0 = 0.75$, $\Delta = 0.7$) for $V_{S,tot} = 40K$. We report some data also for $V_{S,tot} = 60K$ (encircled points) and best fits to Eq. (2).

obtained for $\langle \lambda_n \rangle$ on this single slice are reported, for a few values of n , in Fig. 2, V_S in this case being the average volume of the single maximal slice: statistical errors are reported but are not appreciable. In this case, a smooth extrapolation to the infinite volume limit is obtained by allowing simple power corrections in V_S^{-1} :

$$\langle \lambda_n \rangle_{V_S} = \langle \lambda_n \rangle_{\infty} + \frac{a_n}{V_S} + \frac{b_n}{V_S^2} \quad (3)$$

and $\chi^2/\text{d.o.f.} \simeq 1$ is obtained only allowing for $b_n \neq 0$. As already expected from the results of Ref. [26], the extrapolated values $\langle \lambda_n \rangle_{\infty}$ are non-zero, as shown in Fig. 2. What is more interesting is that the extrapolated values for different values of n do not coincide, i.e. in the thermodynamical limit the spectrum above the gap seems to be discrete, defining a whole hierarchy of length scales for the geometry of the B phase. Further evidence for this comes from the behavior of the volume-normalized spectral density, which becomes smaller and smaller as $V_S \rightarrow \infty$ in the region above the gap, as expected for a discrete spectrum.

Our interest is however mostly focused on the intermediate phase C_b . As discussed above, the two classes of alternating slices differ mostly at large scales. This is better enlightened by looking at the scaling profiles where the eigenvalues λ_n of the LB operator are reported as a function of the scaling variable n/V_S : as discussed in Ref. [26], such profiles provide information about the effective dimensionality of the spatial triangulations at different scales (smaller values of n/V_S correspond to larger scales), $2/d_{EFF} = d \log \lambda_n / d \log(n/V_S)$. In particular, the development of a gap in the LB operator in the $V_S \rightarrow \infty$ limit corresponds to an infinite dimensionality at large scales, induced by a high connectivity of the dual graph. In Fig. 3 we report the profiles obtained in the C_b phase at $k_0 = 0.75$ and for three different values of $\Delta = 0.2, 0.4$ and 0.6 : the point where two differ-

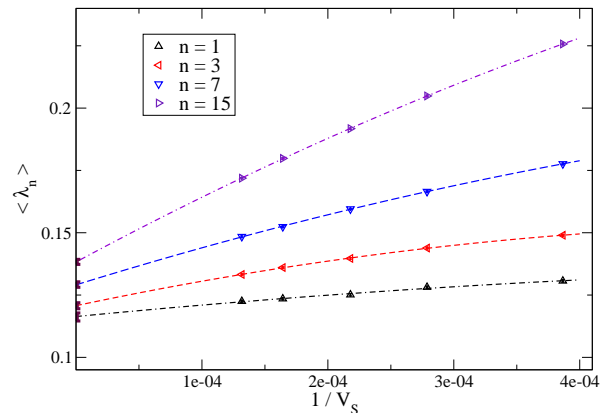


FIG. 2. Average eigenvalues as a function of $1/V_S$ in phase B ($k_0 = 1.0$, $\Delta = -0.2$). Data points at $1/V_S = 0$ are the results of the extrapolation according to Eq. (3).

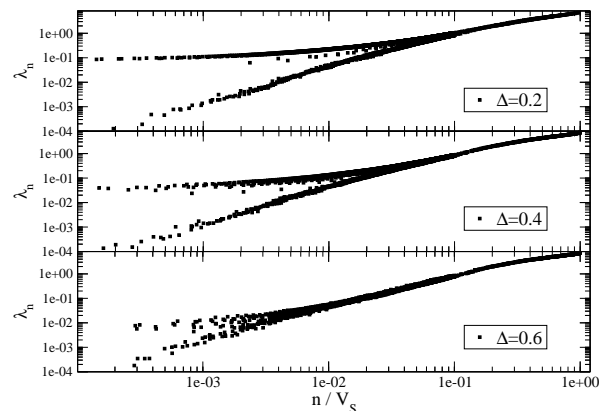


FIG. 3. Scatter plot of λ_n versus n/V_S for the slices (with spatial volume $V_S > 200$) of single configurations sampled at $k_0 = 0.75$, and for three different values of Δ in the C_b phase.

ent profiles emerge moves to smaller and smaller values of n/V_S as Δ moves towards the transition to the C_{ds} phase, where the separation in two classes disappears.

For each of the lowest lying eigenvalues we have computed $\langle \lambda_n \rangle(V_S)$ separately for the two classes of slices, starting from V_S large enough to make the separation unambiguous as in Fig. 3. As an example, in Fig. 4 we report results obtained for $k_0 = 0.75$ and $\Delta = 0.4$ for dS -like slices: the $V_S \rightarrow \infty$ extrapolation can be performed according to Eq. (2) in all cases, with $\chi^2/\text{d.o.f.} \simeq 1$, confirming the absence of a gap.

On the contrary, results for B -like slices, which are reported for the same set of parameters in Fig. 5, clearly point to a non-zero $V_S \rightarrow \infty$ extrapolation, $\langle \lambda_n \rangle_{\infty} \neq 0$. Extrapolated values reported in the figure have been obtained fitting data according to Eq. (3), the reported errors include the systematic uncertainty related to the change of the fitted range or the inclusion or exclusion of the $1/V_S^2$ term. Even taking these systematics into account, one notices that the $\langle \lambda_n \rangle_{\infty}$ values for different n

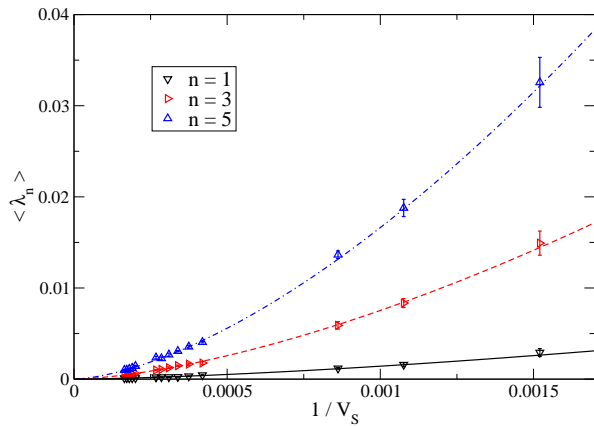


FIG. 4. $\langle \lambda_n \rangle(V_S)$ for dS -like slices in C_b phase ($k_0 = 0.75$, $\Delta = 0.4$, $V_{S,tot} = 40K$). We report also best fits to Eq. (2).

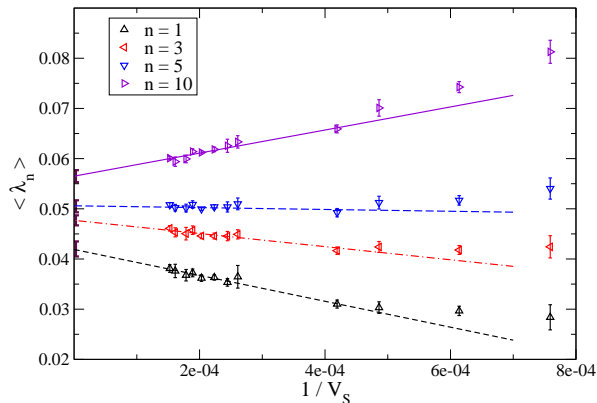


FIG. 5. As in Fig. 4, for B -like slices. We report also some $V_S \rightarrow \infty$ extrapolations with $1/V_S$ corrections (see text).

are not compatible, confirming that also for B -like slices the lowest lying part of the spectrum is likely discrete even in the thermodynamical limit, as for the B phase.

The main point of our investigation is to adopt the non-zero $\langle \lambda_n \rangle_\infty$ of B -like slices as order parameters approaching zero at the $C_b - C_{dS}$ transition and probing the scaling properties associated with a possible critical point there. To that purpose, in Fig. 6 we report the values obtained for some $\langle \lambda_n \rangle_\infty$ ($n = 1$ and 5) as a function of Δ along two different lines ($k_0 = 0.75$ and $k_0 = 1.5$), crossing the $C_b - C_{dS}$ transition line in different points. On dimensional grounds, different $\langle \lambda_n \rangle_\infty$ correspond to different inverse squared lengths, which in the presence of a critical point should scale according to the same critical behavior. Based on this expectation, we have tried a fit according to the scaling formula

$$\langle \lambda_n \rangle_\infty = A_n (\Delta - \Delta_c)^{2\nu} \quad (4)$$

where only the A_n coefficients depend on n . A combined fit, including $n = 1$ and $n = 5$, yields $\Delta_c = 0.635(14)$, $\nu = 0.55(4)$ for $k_0 = 0.75$ ($\chi^2/\text{d.o.f.} = 31/26$), and $\Delta_c = 0.544(36)$, $\nu = 0.82(12)$ for $k_0 = 1.50$ ($\chi^2/\text{d.o.f.} = 6/14$).

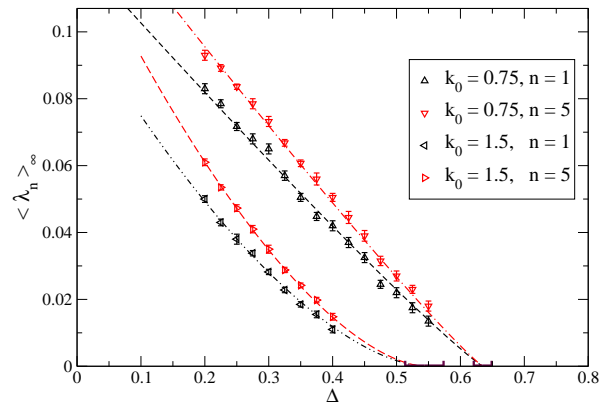


FIG. 6. $\langle \lambda_n \rangle_\infty$ in B -like slices as a function of Δ for different values of k_0 and n , together with best fits to Eq. (4).

Similar and consistent results are obtained including different values of n , or if the eigenvalues are fitted separately; some tension starts to emerge only when eigenvalues with $n \gtrsim 10$ are included. The values of Δ_c are consistent with those obtained analyzing other parameters, based on counting the coordination number of triangulations, introduced in Ref. [29]. Our best fits suggests that the critical index ν could change along the transition line, however we stress that a global fit, in which the index is forced to be the same for both k_0 , works equally well, yielding $\nu = 0.59(4)$, $\Delta_c(k_0 = 0.75) = 0.656(15)$, $\Delta_c(k_0 = 1.5) = 0.479(10)$ with $\chi^2/\text{d.o.f.} = 47/41$.

Concluding remarks - We have shown that, for B -like slices in the C_b phase, as well as for the B phase, the thermodynamical limit of the lowest part of the spectrum of the LB operator suggests the existence of a discrete set of inverse squared lengths. They cannot be considered as proper correlation lengths, but rather as finite length scales which characterize the geometry of the slices even when $V_S \rightarrow \infty$, and have a dependence on the bare parameters which is consistent with a common critical behavior as the transition to the de Sitter phase is approached.

Our results still do not confirm that the gap vanishes continuously. Indeed, our determinations of $\langle \lambda_n \rangle_\infty$ stop well before Δ_c , since volumes where eigenvalues of B -like and dS -like slices are clearly distinguished grow as the C_{dS} phase is approached, so that we could not reliably extrapolate to $V_S = \infty$ close enough to the transition. This happens, for instance, for $\Delta = 0.6$ shown in Fig. 3: yet, even in this case it is clear that a gap still exists and is consistent with the critical fit reported in Fig. 6. Future studies, employing larger values of $V_{S,tot}$, will better clarify the nature of the possible critical behavior of CDT; moreover, studies at different values of k_0 will clarify if the critical behavior actually changes along the transition line.

Acknowledgements Numerical simulations have been performed on the MARCONI machine at CINECA,

based on the agreement between INFN and CINECA (under project INF18_npqcd) and at the IT Center of the Pisa University. We thank in particular M. Davini for his technical support.

-
- * giuseppe.clemente@pi.infn.it
 † massimo.delia@unipi.it
 ‡ alessandro.ferraro@pi.infn.it
- [1] M. H. Goroff, A. Sagnotti, Nucl. Phys. B **266** (1986) 709.
 [2] S. Weinberg, General Relativity, an Einstein Centenary Survey, ch.16 (Cambridge Univ. Press, 1979).
 [3] D. F. Litim, Phil. Trans. Roy. Soc. Lond. A **369** (2011) 2759 [arXiv:1102.4624 [hep-th]].
 [4] M. Reuter, Phys. Rev. D **57** (1998) 971 [hep-th/9605030].
 [5] M. Reuter and F. Saueressig, New J. Phys. **14** (2012) 055022 [arXiv:1202.2274 [hep-th]].
 [6] A. Bonanno and M. Reuter, Phys. Rev. D **65** (2002) 043508 [hep-th/0106133].
 [7] T. Regge, Nuovo Cim. **19**, 558 (1961).
 [8] J. Ambjorn and J. Jurkiewicz, Phys. Lett. B **278**, 42 (1992).
 [9] M. E. Agishtein and A. A. Migdal, Mod. Phys. Lett. A **7**, 1039 (1992).
 [10] J. Ambjorn, J. Jurkiewicz and C. F. Kristjansen, Nucl. Phys. B **393** (1993) 601 [hep-th/9208032].
 [11] T. Rindlisbacher and P. de Forcrand, JHEP **1505** (2015) 138 [arXiv:1503.03706 [hep-lat]].
 [12] J. Laiho, S. Bassler, D. Coumbe, D. Du and J. T. Neelakanta, Phys. Rev. D **96** (2017) no.6, 064015 [arXiv:1604.02745 [hep-th]].
 [13] J. Ambjorn, A. Goerlich, J. Jurkiewicz and R. Loll, Phys. Rept. **519**, 127 (2012) [arXiv:1203.3591 [hep-th]].
 [14] J. Ambjorn, J. Jurkiewicz and R. Loll, Phys. Rev. Lett. **85** (2000) 924 [arXiv:hep-th/0002050].
 [15] J. Ambjorn, S. Jordan, J. Jurkiewicz and R. Loll, Phys. Rev. Lett. **107** (2011) 211303 [arXiv:1108.3932 [hep-th]].
 [16] J. Ambjorn, S. Jordan, J. Jurkiewicz and R. Loll, Phys. Rev. D **85** (2012) 124044 [arXiv:1205.1229 [hep-th]].
 [17] J. Ambjorn, J. Gizbert-Studnicki, A. Goerlich, J. Jurkiewicz, N. Klitgaard and R. Loll, Eur. Phys. J. C **77** (2017) no.3, 152 [arXiv:1610.05245 [hep-th]].
 [18] J. Ambjorn, D. Coumbe, J. Gizbert-Studnicki, A. Goerlich and J. Jurkiewicz, Phys. Rev. D **95** (2017) no.12, 124029 [arXiv:1704.04373 [hep-lat]].
 [19] J. Ambjorn, J. Gizbert-Studnicki, A. Goerlich, K. Grosvenor and J. Jurkiewicz, Nucl. Phys. B **922** (2017) 226 [arXiv:1705.07653 [hep-th]].
 [20] E. Minguzzi and M. Sanchez, EMS Pub.House, 2008, p.299-358 [gr-qc/0609119].
 [21] S. Jordan and R. Loll, Phys. Rev. D **88** (2013) 044055 [arXiv:1307.5469 [hep-th]].
 [22] J. Ambjorn, J. Gizbert-Studnicki, A. Goerlich, J. Jurkiewicz and D. Nemeth, JHEP **1806** (2018) 111 [arXiv:1802.10434 [hep-th]].
 [23] J. Ambjorn, J. Gizbert-Studnicki, A. Goerlich and J. Jurkiewicz, JHEP **1406**, 034 (2014) [arXiv:1403.5940 [hep-th]].
 [24] D. N. Coumbe and J. Jurkiewicz, JHEP **1503**, 151 (2015) [arXiv:1411.7712 [hep-th]].
 [25] J. Ambjorn, J. Jurkiewicz, and R. Loll, Phys.Rev.Lett., 95:171301, (2005) [hep-th/0505113].
 [26] G. Clemente and M. D'Elia, Phys. Rev. D **97**, no. 12, 124022 (2018) [arXiv:1804.02294 [hep-th]].
 [27] C. Sanderson and R. Curtin, Journal of Open Source Software, Vol. 1, pp. 26, 2016.
 [28] A. Goerlich, arXiv:1111.6938 [hep-th].
 [29] J. Ambjorn, D. N. Coumbe, J. Gizbert-Studnicki and J. Jurkiewicz, JHEP **1508**, 033 (2015) [arXiv:1503.08580 [hep-th]].